Measurement of roughness based on Talbot effect in reflection from rough surfaces

Masoomeh Dashtdar,[1,*], Ali Mohammadzade[1] and S. Mohammad-Ali Hosseini-Saber[1]

[1] *Department of Physics, Shahid Beheshti University, Evin, Tehran, Tehran 19839 Iran*

[*] *Corresponding author: m-dashtdar@sbu.ac.ir*

In the present work, the reflected light scattering from a rough surface is studied in the Fresnel diffraction limit, by using a square grating. It is shown theoretically that the scattered light intensity depends on statistical properties of the rough surface, the light incident angle, the grating period, and a geometric coefficient, related to the ratio of distance of the rough surface and the observation plane from the grating. At Talbot distances of the grating, the surface height difference function in terms of multiplication of the Talbot number, the grating period, and the geometric coefficient is the modulation transfer function (MTF) of the scattering in reflection from the rough surface. If the multiplication is larger than twice the surface correlation length, the height difference function is constant for different spatial frequencies, therefore, the square wave is reproduced with smaller contrast. The surface roughness can be obtained by measuring the contrast at different incident angles. It is also shown that the contrast measurements in reflection and transmission provide the refractive index of transparent samples with a rough surface. In experimental studies the roughness of three metal standard rough surfaces are determined in different incident angles. Also, the refractive index of a sheet glass with a rough surface is obtained. The results are quite consistent.

OCIS codes: 290.5880, 070.6760, 260.1960, 120.3940

1. Introduction

Surface roughness measurement is crucial in several applications, including high-quality optics, production of optical diffusers, thin film components and solar cells, data storage on surfaces, and surface quality control [1–5]. Several methods are available for measuring the surface roughness. Stylus profilometry(SP) [6] and scanning probe microscopy (SPM) can provide the surface morphology, directly. Optical methods, including optical profilometry [7, 8], interferometry [9–11], speckle interferometry [12, 13], and light scattering [14–20] have been used, as non contact methods, for roughness measurements. The methods based on light scattering do have relevant advantages: such as the nondestructive methodology, large sampling size, and the capability to provide real-time measurements [21, 22].

In most of the works on light scattering from rough interfaces, the measurement of the coherently or diffusely scattered light intensity, in far field approximation, leads to determination of the surface roughness [23–32]. However, in principle, measurement of these parameters is not straightforward.

In our previous report [33], based on Fresnel diffraction theory, the transmitted light scattering from a randomly rough interface is studied by projection a periodic light intensity distribution on the interface. We showed that the scattered light intensity in Fresnel regime depends on statistical properties of the rough interface and the light intensity period. The self-images contrast exponentially depends on the interface height-height correlation function in terms of multiplication of the self-image number and the period of the light intensity distribution. We applied the approach to determine the roughness of the interfaces by several square gratings with periods much longer than the correlation lengths. The samples were prepared by roughening the sheet glasses by powders of different greet numbers. The results by different gratings and light wavelengths were quite consistent. Since this method is based on determination of the contrast, it is more applicable and accurate than intensity measurements. It doesn't also need a smooth reference sample. However, the problems in transmission mode are that the roughness can be only determined for transparent materials and the refractive index of the sample must be known. These are avoidable in reflection measurements.

The theoretical considerations in reflection reveal that the optical path difference, due to the height distribution, can be changed simply by varying the incident angle, thus low roughnesses can be measured more accuracy at small incident angles and increasing the incident angles provides the possibility of measuring higher roughnesses. Also, measurements in both reflection and transmission can be used for specifying the refractive index of the samples that have rough interfaces such as thin films.

This paper is organized as follows: In Section 2, we introduce the theoretical approaches and calculate the near-field scattered light intensity in reflection from a rough surface by a square grating. We show that, at Talbot distances of the grating, the surface height difference function can be defined as magnitude response of scattering to different spatial frequencies. When the argument of the height difference function is larger that twice the surface correlation lengths, the contrast measurements provide the surface roughness. Also, we determine the refractive index in terms of the contrasts in reflection and transmission. The experimental results are presented in section 3. Conclusions of the work are outlined in Section 4.

2. Theoretical approach

Considering a monochromatic parallel beam of light after passing through a square grating is incident on randomly rough surface, at angle θ. The square grating is located perpendicular to the incident light beam in $\xi - \eta$ plane, Fig. 1. The amplitude transmittance of the grating with a period d, whose direction is parallel to the η-axis, is

$$g(\xi, \eta) = \frac{1}{2}\left[1 + v_0 \sum_{n=1}^{\infty} c_n \cos(\frac{2n\pi\xi}{d})\right], \tag{1}$$

where $0 \leq v_0 \leq 1$ denotes a contrast of the grating in amplitude and $c_n = 4\sin(n\pi/2)/(n\pi)$ is the Fourier coefficient of the grating.

Applying the Fresnel-Kirchhoff integral [34], we calculate the diffracted complex amplitude at point P on $x-y$ plane, that is perpendicular to the specular reflected direction. Considering Fig. 1 the amplitude at point P is similar to the Fresnel-Kirchhoff integral at point P$''$ in the $x'' - y''$ plane (the image of $x - y$ plane) at the distance $z = R_1 + R_2$, however, only the reflectance from the rough surface must be considered. The amplitude of reflected light from the height $h = h(x', y')$ on the rough surface is

$$r(x', y') = a \exp(2ikh \cos\theta), \tag{2}$$

where, a is the reflected amplitude from the unit area of the mean plane and $k = 2\pi/\lambda$ is the light wavenumber. Therefore, the diffracted amplitude from the rough surface can be given by [34]

$$\psi(x, y) = \frac{e^{ikz}}{i\lambda z} \int\int r(x'_1, y'_1) g(\xi, \eta) \exp\left\{\frac{-ik}{2z}\left[(x-\xi)^2 + (y-\eta)^2\right]\right\} d\xi d\eta, \tag{3}$$

By substituting Eqs. (1) and (2) in Eq. (3), the intensity is obtained as

$$\begin{aligned} \langle I(x,y)\rangle &= \langle \psi^*(x,y)\psi(x,y)\rangle = \frac{a^2}{4\lambda^2 z^2}\int\int\int\int \langle \exp\left[2ik\cos\theta(h(x'_1,y'_1) - h(x'_2,y'_2))\right]\rangle \\ &\times \Big[1 + v_0^2 \sum_{n=1}^{\infty}\sum_{m=1}^{\infty} c_n c_m \cos\big(\frac{2n\pi\xi}{d}\big)\cos\big(\frac{2m\pi\xi'}{d}\big) + v_0 \sum_{n=1}^{\infty} c_n \cos\big(\frac{2n\pi\xi}{d}\big) \\ &+ v_0 \sum_{m=1}^{\infty} c_m \cos\big(\frac{2m\pi\xi'}{d}\big)\Big] \exp\left\{\frac{+ik}{2z}\left[(x-\xi)^2 + (y-\eta)^2\right]\right\} \\ &\times \exp\left\{\frac{-ik}{2z}\left[(x-\xi')^2 + (y-\eta')^2\right]\right\} d\xi d\eta d\xi' d\eta', \end{aligned} \tag{4}$$

where $\langle \exp\big[2ik\cos\theta\big(h(x_1',y_1')-h(x_2',y_2')\big)\big]\rangle$ is the height difference function in reflection from the rough surface. It is a function of two-point separation on the rough surface that can be shown as $\chi(x_1'-x_2',y_1'-y_2')$ (the brackets indicate averaging over the whole surface of interest) [14]. Considering Fig. 1, one can write

$$
\begin{aligned}
x_1'-x_2' &= \alpha(\xi-\xi') \\
y_1'-y_2' &= \beta(\eta-\eta'),
\end{aligned}
\tag{5}
$$

where, $\alpha = R_2/(z\cos\theta)$ and $\beta = R_2/z$. According to Eq. (5) and changing the variables $\xi-\xi' = X$, $\xi+\xi' = Y$, $\eta-\eta' = X'$, and $\eta+\eta' = Y'$, the scattered intensity is given by

$$
\begin{aligned}
\langle I(x,y)\rangle &= \frac{a^2}{16\lambda^2 z^2}\sum_{n=1}^{\infty}\sum_{m=1}^{\infty}\int\int\int\int \chi(\alpha X,\beta X') \\
&\times \Big\{1+v_0^2 c_n c_m \cos\big[\frac{n\pi(X+Y)}{d}\big]\cos\big[\frac{m\pi(X-Y)}{d}\big] \\
&+ v_0 c_n \cos\big[\frac{n\pi(X+Y)}{d}\big]+v_0 c_m \cos\big[\frac{m\pi(X-Y)}{d}\big]\Big\} \\
&\times \exp\big[\frac{+ik}{2z}\,(XY+X'Y'-2Xx-2X'y)\big]dXdYdX'dY'.
\end{aligned}
\tag{6}
$$

By using the property of Dirac' s delta function and performing the integrations, Eq. (6) leads to

$$
\begin{aligned}
\langle I(x,y)\rangle &= \frac{I_0}{4}\Big\{\chi(0,0)+2v_0\sum_{n=1}^{\infty}c_n\chi(\frac{n\alpha\lambda z}{d},0)\cos(\frac{2n\pi x}{d})\cos(\frac{n^2\pi\lambda z}{d^2}) \\
&+ \frac{v_0^2}{2}\sum_{n=1}^{\infty}\sum_{m=1}^{\infty}c_n c_m\cos\big(\frac{\pi\lambda z(m^2-n^2)}{d^2}\big) \\
&\times \Big[\chi(\frac{\alpha\lambda z(m-n)}{d},0)\cos\big(\frac{2\pi x(m-n)}{d}\big) \\
&+ \chi(\frac{\alpha\lambda z(m+n)}{d},0)\cos\big(\frac{2\pi x(m+n)}{d}\big)\Big]\Big\},
\end{aligned}
\tag{7}
$$

where $I_0 = a^2$. Since the normalized height distribution is considered for rough interfaces, $\chi(0,0) = 1$. Further, the spatial stationary situation provides $\chi(X,0) = \chi(X)$. Then Eq. (7) becomes

$$
\begin{aligned}
\langle I(x,y)\rangle &= \frac{I_0}{4}\Big\{1+2v_0\sum_{n=1}^{\infty}c_n\chi(\frac{n\alpha\lambda z}{d})\cos(\frac{2n\pi x}{d})\cos(\frac{n^2\pi\lambda z}{d^2}) \\
&+ \frac{v_0^2}{2}\sum_{n=1}^{\infty}\sum_{m=1}^{\infty}c_n c_m\cos\big(\frac{\pi\lambda z(m^2-n^2)}{d^2}\big) \\
&\times \Big[\chi(\frac{\alpha\lambda z(m-n)}{d})\cos\big(\frac{2\pi x(m-n)}{d}\big) \\
&+ \chi(\frac{\alpha\lambda z(m+n)}{d})\cos\big(\frac{2\pi x(m+n)}{d}\big)\Big]\Big\}.
\end{aligned}
\tag{8}
$$

At Talbot distances, $z = d^2N/\lambda$ for N taking integers, the intensity is obtained as

$$\begin{aligned}\langle I(x,y)\rangle &= \frac{I_0}{4}\Big\{1 \pm 2v_0\sum_{n=1}^{\infty} c_n\chi(n\alpha Nd)\cos(\frac{2n\pi x}{d}) + \frac{v_0^2}{2}\sum_{n=1}^{\infty}\sum_{m=1}^{\infty} c_nc_m \\ &\times \Big[\chi(\alpha Nd(m-n))\cos\big(\frac{2\pi x(m-n)}{d}\big) \\ &+ \chi(\alpha Nd(m+n))\cos\big(\frac{2\pi x(m+n)}{d}\big)\Big]\Big\},\end{aligned} \tag{9}$$

$(+)$ and $(-)$ denote even and odd values of N, respectively. The coefficient of cosine, in Eq. (9), is given by height difference function, that can be defined as magnitude response of scattering in reflection from the rough surface to sinusoids of different spatial frequencies; that is the modulation transfer function (MTF). The height difference function in reflection, for a Gaussian height distribution at incident angle θ, is [14, 35]

$$\chi(X) = \exp\big(-2k^2\cos^2\theta H(X)\big), \tag{10}$$

where $H(X)$ is the height-height correlation function that has the following form:

$$H(X) = 2\sigma^2\big(1 - C(X)\big), \tag{11}$$

where σ is the rms height distribution and $C(X)$ is the height correlation function of the rough surface. The height correlation function is usually assumed as a Gaussian function, $C(X) = \exp(-X^2/\lambda_0^2)$, or decreasing exponential function, $C(X) = \exp(-|X|/\lambda_0)$, where λ_0 is the correlation length [14, 36]. In Fig. 2, the height difference functions in reflection from rough surfaces, having the Gaussian correlation functions with different roughnesses, are plotted versus X/λ_0, for normal incident angle. For values of $X/\lambda_0 \geq 2$ the height difference function doesn't change and only dependent on the surface roughness. In Fig. 3(a), the normalized intensity ($\langle I(x,y)\rangle/I_0$) variation of a square grating with a period of $d = 0.2$ mm ($N = 0$) and scattered from a rough surface of $\lambda_0 = 4d$ and $\sigma = 0.13\lambda$, for $\alpha = 1/2$ and normal incident angle, are shown in different Talbot distances. At first Talbot distance, the contrast is still unity, but the square wave is not well reproduced. By increasing the Talbot numbers, the contrast decreases, and at higher spatial frequencies there is more reduction in the Talbot images. When the number of the Talbot images increases enough that the height difference function is same for different spatial frequencies, the square wave is reproduced. However, for surfaces with higher roughness so that the height difference function is vanish, the Talbot image is not constructed, Fig. 3(b) (same as Fig. 3(a), but, for $\sigma = 0.2\lambda$).

For values of αNd longer than twice the correlation length the height difference function is constant for different spatial frequencies and Talbot distances, that can be obtained by substituting Eq. (11) in to Eq. (10) for $C(\alpha Nd) = 0$. Therefore, according to Eq. (9) the contrast of the Talbot images is

$$V = \frac{2v_0 \exp\left(-4k^2 \cos^2\theta \sigma^2\right)}{1+v_0^2}. \tag{12}$$

In the previous report [33], the contrast of the transmitted scattering light at the Talbot images of the square periodic light intensity on a rough interface, with periods longer than twice the interface correlation length, was obtained as

$$V_t = \frac{2v_0 \exp\left[-k^2(n-1)^2\sigma^2\right]}{1+v_0^2}, \tag{13}$$

where n is the relative refractive index of media on both sides of the rough interface. By substituting σ from Eq. (12) into Eq. (13), the refractive index can be obtained as

$$n = 1 + 2\cos\theta\sqrt{\frac{\ln[(1+v_0^2)V_t - \ln(2v_0)]}{\ln[(1+v_0^2)V - \ln(2v_0)]}}. \tag{14}$$

3. Experimental procedures and results

The scheme of experimental setup is shown in Fig. 4. An expanded beam of a He-Ne laser ($\lambda = 633$ nm) illuminates a square grating of period $d = 0.2$ mm at normal incidence. The diffracted light from the grating is incident on the sample at angle θ, that is mounted on a rotating platform at distance R_1 from the grating. A complementary metal-oxide semiconductor (CMOS) (Canon D450) is located perpendicular to the specular reflected direction at distance R_2 from the axis of the sample platform, so that $z = R_1 + R_2$ is equal to the second grating Talbot distance ($2d^2/\lambda$). The incident and reflected angles could be fixed to a precision of 0.1 degree. The samples are three metal ground rough surfaces of a roughness standard (Rugotest 104), with the rms of the height distributions of 0.06, 0.1, and 0.2 microns. In Fig. 5 the intensity distributions recorded by the CMOS are shown at Talbot distance of the grating (reference) [Fig. 5(a)] and for reflected from the sample of roughness $\sigma = 0.1\ \mu m$ at incident angles 65°, 50°, and 40° in Figs. 5(b)-5(d), respectively. Figs. 5(a')-5(d') are the corresponding average intensity distribution along the grating lines. In Eq. (12) v_0 can be obtained from the calculation of the contrast of intensity distribution at Talbot distance of the grating. Therefore measurement of the contrast of light intensity distribution reflected from the rough surface in different incident angles yield the surface roughness. The corresponding calculated roughnessses with the associated errors are listed in Table 1. The errors are obtained by repeating the experiments. For incident angles smaller than 65°, the Talbot image of the scattered light from the sample with $\sigma = 0.2\ \mu m$ is not constructed.

In order to show the ability of the present approach to determine the refractive index of transparent materials with a rough interface, we used a sample of sheet glass of dimensions $50 \times 50 \times 4$ mm and refractive index $n = 1.532 \pm 0.008$. The refractive index of the sample was obtained by the method described in Ref. [37]. After measuring the refractive index, one face of the sample is roughened by a powder of 3000 grit number. In Fig. 6(a) the intensity distribution of the reflected light from the sample are shown at incident angle 80°. We also performed the experiments in transmission mode [33]. In Fig. 6(b), the light intensity distribution is shown at the Talbot distance from the grating after transmitting from the rough surface of the sample, at normal incidence. Figs. 6(a') and 6(b') are the corresponding average intensity distribution along the grating lines. According to Eq. (14), the refractive index can be defined by calculation of the contrast in reflection, at different incident angles, and in transmission, at normal incident. The corresponding refractive index is 1.528 ± 0.003 that is in good agreement with the refractive index of the sheet glass.

4. Conclusion

(a) When the diffracted light from a square grating is scattered from a rough surface, the surface height difference function in terms of αNd is the magnitude response of scattering to different spatial frequencies.
(b) For values of $\alpha Nd < 2\lambda_0$, there is more reduction at higher spatial frequencies in the Talbot images. The Talbot images intensity distribution depend on the surface roughness and correlation length.
(c) For values of $\alpha Nd \geq 2\lambda_0$, the height difference function is same for different spatial frequencies, therefore, the square wave is reproduced at Talbot distances. The contrast of the square wave depends on surface roughness and angle of incidence.
(d) The roughness of standard surfaces obtained in different incident angles are quite consistent.
(e) The contrast measurements in reflection and transmission provide the refractive index of transparent samples with a rough surface.

References

1. K. H. Guenther, P. G. Wierer, and J. M. Bennett, "Surface roughness measurements of low-scatter mirrors and roughness standards," Appl. Opt. **23**, 3820–3836 (1984).
2. M. Dashtdar and M. T. Tavassoly, "Transforming a spatially coherent light beam into a diffused beam of small diffusion angle using suitable surface scattering," Opt. Commun. **308** 7–10 (2013).
3. C. Amra, "From light scattering to the microstructure of thin-film multilayers ," Appl. Opt. **32**, 5481–5491 (1993).
4. C. Rockstuhl, S. Fahr, K. Bittkau, T. Beckers, R. Carius, F.-J. Haug, T.Soderstrom, C. Ballif, and F. Lederer, "Comparison and optimization of randomly textured surfaces in thin-film solar cells ," Opt. Express **18**, A335–A341 (2010).

5. D. J. Whitehouse, "Review Article, Surface metrology," Meas. Sci. Technol. **8**, 955–972 (1997).
6. K. A. O'Donnell, "Effect of finite stylus width in surface contact profilomery," Appl. Opt. **32**, 4922–4928 (1993).
7. Y. Fainman, E. Lenz, and J. Shamir, "Optical profilometer: a new method for high sensitivity and wide dynamic range," Appl. Opt. **21**, 3200–3208 (1982).
8. S. Arhab, G. Soriano, K. Belkebir, A. Sentenac, and H. Giovannini, "Full wave optical profilometry," J. Opt. Soc. Am. A **28**, 576–580 (2011).
9. J. M. Bennett, "Measurement of the rms roughness, autocovariance and other statistical properties of optical surfaces using a FECO scanning interferometer," Appl. Opt. **15**, 2705–2721 (1976).
10. B. Wiesner, O. Hybl, and G. Hausler, "Improved white-light interferometry on rough surfaces by statistically independent speckle patterns," Appl. Opt. **51**, 751–757 (2012).
11. O. V. Angelsky and P. P. Maksimyak, "Optical diagnostics of random phase objects," Appl. Opt. **29**, 2894–2898 (1990).
12. C. J. Tay, S. L. Toh, H. M. Shang, and J. B. Zhang, "Whole-field determination of surface roughness by speckle correlation," Appl. Opt. **34**, 2324–2335 (1995).
13. P. Lehmann, "Surface-roughness measurement based on the intensity correlation function of scattered light under speckle-pattern illumination," Appl. Opt. **38**, 1144–1152 (1999).
14. P. Beckman and A. Spizzochino, *The Scattering of Electromagnetic Wave from Rough Surfaces* (Macmillan, New York, 1963).
15. T. M. Elfouhaily and C. A. Guerin, "A critical survey of approximate scattering wave theories from random rough surfaces," Waves Random Media **14**, R1–40 (2004).
16. A. Krywonos, J. E. Harvey, and N. Choi, "Linear systems formulation of scattering theory for rough surfaces with arbitrary incident and scattering angles," J. Opt. Soc. Am. A **28**, 1121–1138 (2011).
17. O. V. Angelsky, P. P. Maksimyak, V. V. Ryukhtin, and S. G. Hanson, "New feasibilities for characterizing rough surfaces by optical-correlation techniques," Appl. Opt. **40**, 5693–5707 (2001).
18. O. V. Angelsky, D. N. Burkovets, P. P. Maksimyak, and S. G. Hanson, "Applicability of the singular-optics concept for diagnostics of random and fractal rough surfaces," Appl. Opt. **42**, 4529–4540 (2003).
19. W. T. Welford, "Optical estimation of statistics of surface roughness from light scattering measurements," Opt. Quant. Elect. **9**, 269–287 (1977).
20. M. Dashtdar and M. T. Tavassoly, "Roughness measurement using threshold angle of image formation," Opt. Eng. **50**, 123601-1–5 (2011).
21. Y.-P. Zhao, Y.-J. Wu, H.-N. Yang, G.-C. Wang, and T.-M. Lu, "In situ real-time study of chemical etching process of Si(100) using light scattering," Appl. Phys. Lett. **69**, 221–223 (1996).
22. E. Chason, M. B. Sinelair, J. A. Floro, J. A. Hunter, and R. Q. Hwang, "Spectroscopic light scattering for real-time measurements of thin film and surface evolution," Appl. Phys. Lett. **72**, 3276–3278 (1998).
23. H. E. Bennett and J. O. Porteus, "Relation between surface roughness and specular Reflectance at normal incidence," J. Opt. Soc. Am. **51**, 123–129 (1961).

24. P. J. Chandley, "Surface roughness measurements from coherent light scattering," Opt. Quant. Elect. **8**, 323–327 (1976).
25. K. A. O'Donnell and E. R. Mendez, "Experimental study of scattering from characterized random surfaces," J. Opt. Soc. Am. A **4**, 1194–1205 (1987).
26. E. Marx and T. V. Vorburger, "Direct and inverse problems for light scattered by rough surfaces," Appl. Opt. **29**, 3613–3626 (1990).
27. S.-M. F. Nee, R. V. Dewees, T.-W. Nee, L. F. Johnson, and M. B. Moran, "Slope distribution of a rough surface measured by transmission scattering and polarization," Appl. Opt. **39**, 1561–1569 (2000).
28. L.-X. Cao, T.V. Vorburger, A. G. Lieberman, and T. R. Lettieri, "Light scattering measurement of the rms slopes of rough surfaces," Appl. Opt. **30**, 3221–3227 (1991).
29. M. Zamani, S. M. Fazeli,M. Salami, S. Vasheghani Farahani, and G. R. Jafari, "Path derivation for a wave scattered model to estimate height correlation function of rough surfaces," Appl. Phys. Lett. **101**, 141601-1–4 (2012).
30. M. Dashtdar and M. T. Tavassoly, "Redshift and blueshift in the spectra of lights coherently and diffusely scattered from random rough interfaces," J. Opt. Soc. Am. A **26**, 2134–2138 (2009).
31. M. T. Tavassoly and M. Dashtdar, "Height distribution on a rough plane and specularly diffracted light amplitude are Fourier transform pair," Opt. Commun. **281** 2397–2405 (2008).
32. M. Dashtdar and M. T. Tavassoly, "Determination of height distribution on a rough interface by measuring the coherently transmitted or reflected light intensity," J. Opt. Soc. Am. A **25**, 2509–2517 (2008).
33. M. Dashtdar and S. M.-A. Hosseini-Saber, "Determination of the rough interface parameters using the self-imaging effect," J. Opt. Soc. Am. A **30**, 2416–2421 (2013).
34. M. Born and E. Wolf, *Principles of optics* (Cambridge University Press, Cambridge, 2002), pp. 421–430.
35. Y.-P. Zhao, G.-C. Wang, and T.-M. Lu , *Characterization of Amorphous and Crystalline Rough Surface –Principles and Applications (Experimental Methods in the Physical Sciences, Vol. 37)* (Academic Press, 2001) pp. 133–156.
36. J. A. Ogilvy, *Theory of Wave Scattering from Random Rough Surfaces* (Adam Hilger, Briston, 1991).
37. M. T. Tavassoly, "A simple method for measuring the refractive index of a plate," Opt. Lasers Eng. **35**, 397–402 (2001).

Table 1. The roughnesses obtained at different incident angles for three metal standard rough surfaces (Rugotest 104), with $\sigma_1 = 0.06\mu m$, $\sigma_2 = 0.1\mu m$, and $\sigma_3 = 0.2\mu m$.

$\theta(deg)$	σ_1 (μ m)	σ_2 (μ m)	σ_3 (μ m)
35°	0.058 ± 0.005	0.102 ± 0.006	$-$
40°	0.056 ± 0.006	0.098 ± 0.006	$-$
45°	0.058 ± 0.004	0.105 ± 0.008	$-$
50°	0.059 ± 0.003	0.10 ± 0.01	$-$
55°	0.059 ± 0.005	0.11 ± 0.01	$-$
60°	0.060 ± 0.006	0.102 ± 0.009	$-$
65°	0.060 ± 0.006	0.10 ± 0.01	0.19 ± 0.03
70°	0.061 ± 0.006	0.10 ± 0.02	0.18 ± 0.04

5. List of Figure Captions

List of Figures

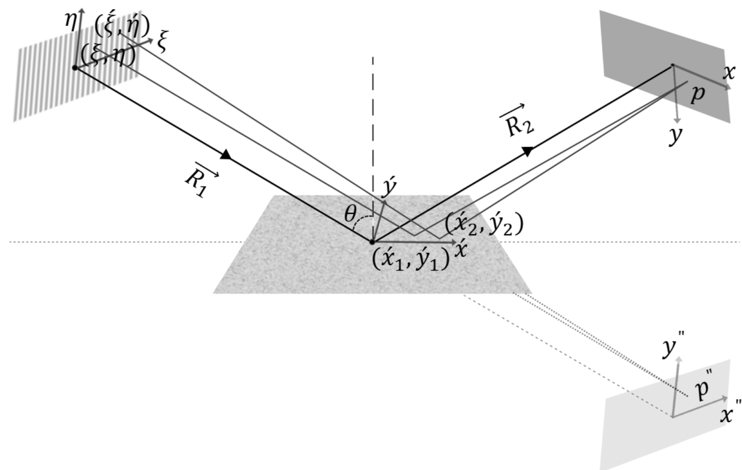

Fig. 1. The geometry used for calculating the diffracted amplitude in reflection from the rough surface by the Fresnel-Kirchhoff integral.

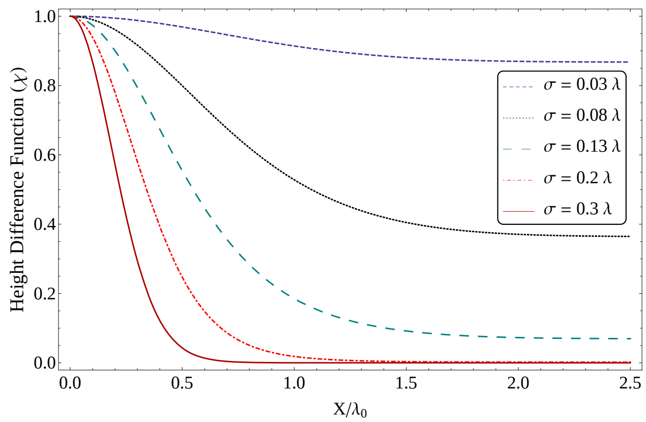

Fig. 2. Height difference functions in reflection from surfaces with five different roughness, at normal incidence, versus X/λ_0.

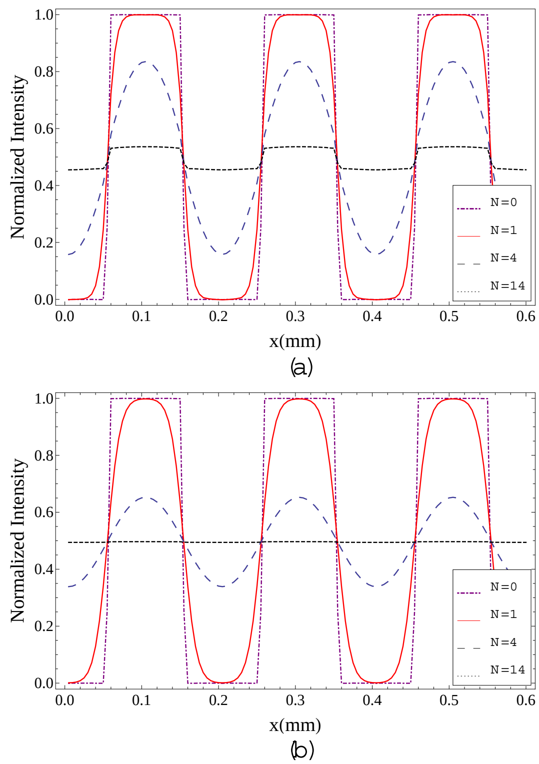

Fig. 3. (a) Normalized intensity variation of a square grating with a period of $d = 0.2$ mm ($N = 0$) and scattered from a rough surface of $\lambda_0 = 4d$ and $\sigma = 0.13\lambda$, for $\alpha = 1/2$ and normal incidence, at different Talbot distances. (b) Same as (a) but for $\sigma = 0.2\lambda$.

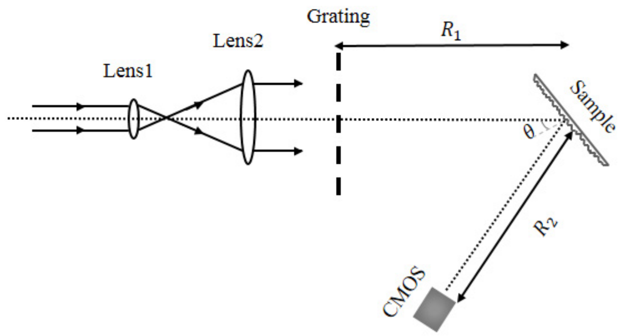

Fig. 4. Experimental setup. An expanded beam of a He-Ne laser after diffracting from the grating is incident on the sample at angle θ. A CMOS records the Fresnel scattered intensity distribution, in the specular reflected direction, at Talbot distance of the grating ($R_1 + R_2 = 2d^2/\lambda$).

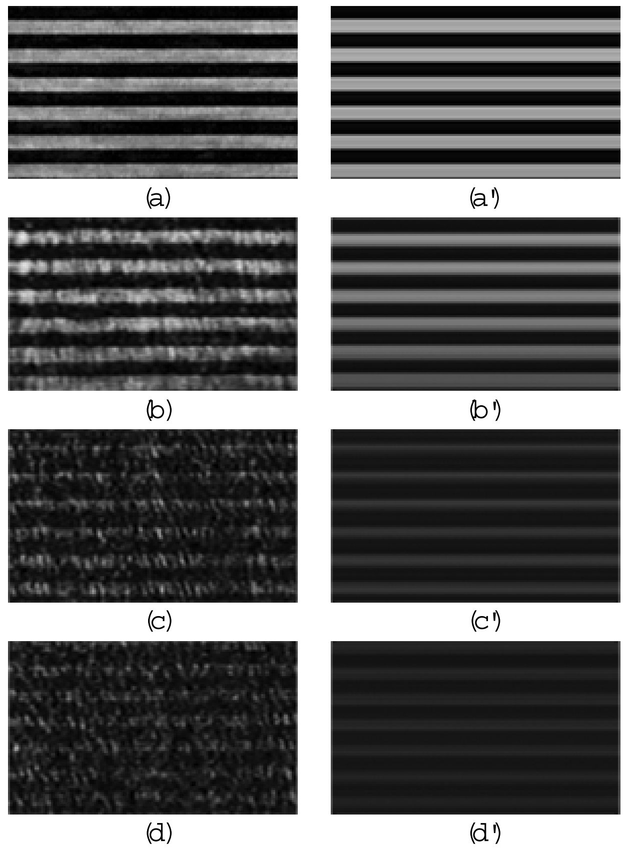

Fig. 5. The intensity distribution at Talbot distance (a) of the grating and for reflected from the sample with $\sigma = 0.1$ μm at incident angles (b) 65°, (c) 50°, and 40°; (a')-(d') the corresponding average intensity distribution along the grating lines.

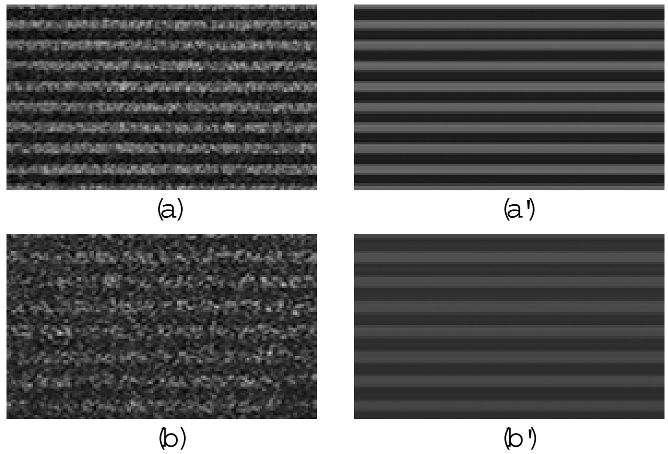

Fig. 6. The intensity distribution at Talbot distance (a) of the reflected light at incident angle 80°, and (b) for the transmitted light at normal incidence from the sample roughened by a powder of 3000 grit number; (a') and (b') the corresponding average intensity distribution along the grating lines.